IJCRT.ORG ISSN : 2320-2882

INTERNATIONAL JOURNAL OF CREATIVE RESEARCH THOUGHTS (IJCRT)

An International Open Access, Peer-reviewed, Refereed Journal

THE CONSEQUENCES OF WALL PROPERTIES AND SLIP ON THE PERISTALTIC MOTION OF JEFFERY LIQUID IN A NON-UNIFORM TUBE WITH HEAT TRANSFER

Mahadev M. Channakote[1] , Dilipkumar V. Kalse[2], Asha S. K[3]

[1,] Department of Mathematics and Statistics, M S Ramaiah University of Applied Sciences Bengaluru, Karnataka 560054, India.

[2]Department of Applied Sciences and Humanities, Guru Nanak Dev Engineering College, Bidar Karnataka 560054, India.

[3]Department of Mathematics, Karnataka University, Dharwad, India.

Email: mchannakote@rediffmail.com, as.kotnur2008@gmail.com

Abstract: This article addresses the influence of viscous dissipation and convective boundary conditions in the peristaltic wave propagation of a Jeffrey fluid in a non-uniform tube. The equations obtained were reduced by using a long-wavelength and a low Reynolds number assumption. Wall properties analysis is also present. The results are visually inspected and briefly discussed after the expression for flow behaviour has been determined. The ambient temperature is shown to rise when the Brinkman number increases. The influence of slip and non-Newtonian factors is investigated using velocity field contours after this paper.

***Keyword* - Jeffrey fluid, peristaltic blood flow, Velocity slip, Thermal slip, Non-uniform tube**

I. INTRODUCTION

Peristaltic motion, which is induced via continuous waveform area relaxation or contraction down the length of an extended conduit, has aroused the curiosity of current fluid dynamics experts. Peristalsis causes many physiological fluids to circulate. Food is absorbed through the esophagus, cell transit in the gastrointestinal system, the mechanism of urine transferring from the kidneys to the urinary bladder, spermatozoa passage in the male reproductive tracts ducts afferents, and vasomotion of tiny blood arteries are all examples of this sort of event. In the oil, industrial, paper, and food sectors and the nuclear, ceramic, and porcelain industries, this is a regular occurrence. Latham (1966) analyzed the peristalsis phenomena in viscous liquids employing analytical and experimental methods first. The moment of viscous material in a channel and a tabular arrangement with peristalsis was examined by Shapiro et al. (1969) A copious investigation on the peristaltic transport of various fluid flow with different geometries under external effects are well reported in the literature (Brasseur (1987), Vasudev, et al. (2011), Asha, et al. (2010, 2019), Mansutti, et al.(1993), Rathod and Mahadev (2011), Naveed Imran et al. (2020), Gijabhare et al. (2019), Narula) et al (2020). In biological systems, the study of non-Newtonian fluids is significant. Three different kinds of non-Newtonian fluids exist; rate type, difference, and integral type. The action of relaxation and retardation times is represented by rate-type fluids. The Maxwell fluid, which shows relaxation time behaviour, is the most basic subclass of rate type material. The behaviour of retardation time is not depicted in this model. As a consequence, the Jeffrey fluid model demonstrates the effect of retardation and relaxation parameters on fluid and heat transfer properties. Further biofluids in the physiological system have been studied to discover a therapy for diagnostic issues during human blood circulation. Numerous models have been developed to report such physiological fluids, but their entire perspective has yet to be realized, and many problems remain unanswered. It is also possible that physiological fluids like blood display both Newtonian and non-Newtonian behaviour simultaneously. Amid these models, the Jeffrey fluid model is essential for both biofluid and polymer sectors. It is well acknowledged that the Jeffrey model is a crucial non-Newtonian model for characterizing blood flow in arteries among the non-Newtonian models. References (Maqbool, 2016, Kavitha et al. (2012), Hanumesh et al. (2017), Nadeem et al. (2013), Akarma et al. (2018), Singh et al.(2018)) include intriguing recent research in this area. The liquid velocity at a solid-liquid contact is not proportional to the solid speed, resulting in slip characteristics at the boundary. This state can be achieved physically by chemically cumulative the hydrophobicity or hydration inclination of the border surface. Slip may also be noticed in rarefied gas motions in micro-electro-mechanical systems (MEMS) technology. Polymer melts frequently exhibit tiny wall slides, showing the insufficiency of the no-slip requirement. Shear skin, squirt, and hysteretic impacts are all influenced by the slip condition. Hayat and Hina (2011) investigated the non-uniform channel flow of Williamson fluid duet to peristalsis. In the context of persuaded slip circumstances, Rathod et al. (2012) reported peristaltic movement of Jeffrey liquid. Hayat et al. (2007) examined asymmetric third-order fluid channel flow generated by peristalsis. Ali et al. (2009) explored the peristaltic action of a third-order liquid in an asymmetric channel. On MHD peristaltic transit, the effects of slip circumstances, wall characteristics, and thermal expansion were analysed by Srinivas et al.(209) Srinivas et al.(2010) showed the slip-induced peristaltic Jeffrey liquid in an asymmetric inclined channel. According to their findings, the amplitude of stress at the upper wall of an asymmetric channel is greater than that of an asymmetric channel.

Heat transfer is shown to have a vital function during fluid flows in fluid mechanics due to its extensive uses in technical and biomedical fields, such as laser therapy, cancer tumour treatment, hypothermia, oxygenation, and hemodialysis. Current research examines the relationships of heat and the transmission of mass with peristalsis. Haemodialysis mechanisms, the destruction of unwanted cancer tissues, oxygenation, medication delivery systems, blood flow convection from tissue pores, and DNA sequences are all examples of applications in this field. The literature on peristalsis has been considered in the last few decades, and few studies in this approach may be consulted. MHD peristaltic flow of Jeffrey fluid in a channel with heat transfer was investigated by Rathod et al. (2014). Peristaltic pumping of fractional second-grade fluid with heat transfer in the vertical cylindrical conduit was examined by Rathod and Mahadev (2014). An investigation of ureteral peristalsis in the canister through porous media was reported by Rathod et al. (2011). Using the multi-step differential transform approach, Wahed et al. (2019) investigated the peristaltic movement of Jeffery fluid under the effect of Joule heat. Asha et al. (2014) addressed the peristalsis with a combined impact of hall and transfer of heat on the MHD Jeffery liquid in a vertical porous conduit. Wall features a study on peristaltic motion of various fluids that has aroused the interest of numerous investigators due to its practical applicability. The enlarged intensity of such effects, in particular, can considerably impact blood pressure in the human body. Mahadev and Dilipkumar (2021) discussed the heat transfer in peristaltic motion of Rabinowistch fluid in a channel with a permeable wall. Kumar et al (2017) examined the sequel of the slip-on peristaltic mechanism of Rabinowitsch fluid in a tube. Sadaf and Nadeem (2017) addressed the peristaltic activity of the Rabinowitsch viscoelastic fluid in the diverging tube with viscous dissipation and convective sequel. Kumar et al. (2013) explored the character of heat flow on pumping mechanism owing to peristalsis in a conduit with wall attributes using a Jeffrey liquid model.

The velocity and temperature properties of peristaltic flow of a fluid flow through a non-uniform tube are yet to be investigated based on the aforementioned literature. As a result, the current work concentrated on the peristaltic pumping of a Jeffrey liquid via a non-uniform tube. Slip, convective effects, and wall characteristics are all taken into account. For the velocity and temperature expression, a closed-form of solutions is developed. Graphs and analyses of the impacts of various flow factors are shown.

I. Mathematical Formulation

The peristaltic action of a non-Newtonian (Jeffrey) fluid in a cylindrical diverging conduit of radius a is analyzed in the presence of slip (see Figure 1). The axisymmetric inertia free flow in the cylindrical tube is generated by sinusoidal wave propagation with wave speed. The mathematical representation of the wall geometry is:

$$H^*(z,t) = a(z^*) + b\sin\frac{2\pi}{\lambda}(z^* - Ct^*),\ a(z^*) = a_2 + kz^*. \tag{2.1}$$

Where $H^*$the mathematical form of the wave with a non-uniform radius is $a(z^*)$, b is the amplitude, λ is the wavelength. The ensuing equations for Jeffery liquid are as follows

$$\left.\begin{aligned} T^* &= p\,I^* + S^* \\ S^* &= \frac{\mu}{1+\lambda_1}(\dot{\gamma} + \lambda_2\ddot{\gamma}) \end{aligned}\right\} \tag{2.2}$$

where S^* is the extra tensor, T^* is the Cauchy's stress tensor, λ_1 is the ratio of relaxation to retardation time, λ_2 is the deceleration time, I^* is the identity tensor and γ is the shear rate and dots over the γ label differentiation concerning time.

The following are the basic equations for the flow problem:

$$\frac{1}{r^*}\frac{\partial(r^* u^*)}{\partial r^*}+\frac{\partial w^*}{\partial z^*}=0, \tag{2.3}$$

$$\rho\left(\frac{\partial u^*}{\partial t^*}+u^*\frac{\partial u^*}{\partial r^*}+w^*\frac{\partial u^*}{\partial z^*}\right)=-\frac{\partial p^*}{\partial r^*}+\frac{1}{r^*}\frac{\partial(r^*\tau_{r^*r^*})}{\partial r^*}+\frac{\partial \tau_{r^*z^*}}{\partial z^*}-\frac{\tau_{\theta^*\theta^*}}{r^*}, \tag{2.4}$$

$$\rho\left(\frac{\partial w^*}{\partial t^*}+u^*\frac{\partial w^*}{\partial r^*}+w^*\frac{\partial w^*}{\partial z^*}\right)=-\frac{\partial p^*}{\partial z^*}+\frac{1}{r^*}\frac{\partial(r^*\tau_{r^*z^*})}{\partial r^*}+\frac{\partial(\tau_{z^*z^*})}{\partial z^*}, \tag{2.5}$$

$$\rho c_p\left(\frac{\partial T^*}{\partial t^*}+u^*\frac{\partial T^*}{\partial r^*}+w^*\frac{\partial T^*}{\partial z^*}\right)=k_1\left(\frac{\partial^2 T^*}{\partial r^{*2}}+\frac{1}{r^*}\frac{\partial T^*}{\partial r^*}+\frac{\partial^2 T^*}{\partial z^{*2}}\right)$$

$$+\tau_{r^*r^*}\frac{\partial u^*}{\partial r^*}+\tau_{z^*z^*}\frac{\partial u^*}{\partial z^*}+\tau_{r^*z^*}\left(\frac{\partial w^*}{\partial r^*}+\frac{\partial u^*}{\partial z^*}\right). \tag{2.6}$$

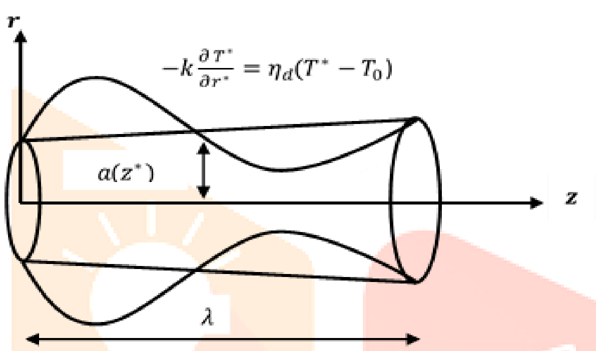

Figure 1 Geometry of the flow

In the transverse coordinates, $u^*$and w^* are the velocity components, respectively ρ, density, p is pressure, T is temperature, k_1 is thermal conductivity, c_p is specific heat, t^* is time, $\tau_{r^*r^*}, \tau_{r^*z^*}, \tau_{z^*z^*}$ are extra stress tensor components.

The following are some relevant boundary conditions for the research concern problem:

$$w^*=-c+\beta\frac{\partial w^*}{\partial r^*}\ at\ r^*=H^*,\ \frac{\partial w^*}{\partial r^*}=0\ \ at, r^*=0\,, \tag{2.7}$$

$$-k_1\frac{\partial T^*}{\partial r^*}=\eta_d(T^*-T_0^*)\ at\ r^*=H^*,\quad \frac{\partial T^*}{\partial r^*}=0\ \ at, r^*=0. \tag{2.8}$$

We introduce the following non-dimensional parameters:

$$w=\frac{w^*}{c}, u=\frac{u^*}{c\delta}, z=\frac{z^*}{\lambda}, r=\frac{r^*}{a_2}, \delta=\frac{a_2}{\lambda}, p=\frac{p^* a_2^2}{\mu\, c\, \lambda}, Re=\frac{\rho\, c\, a_2}{\mu}, \theta=\frac{T^*-T_0}{T_0}, t=\frac{ct^*}{\lambda}\ ,\ \phi=\frac{b}{a_2}, \tau_{i,j}=\frac{a_2\tau_{i,j}^*}{c\mu},$$

$$a(z^*)=a_2+kz^*, h=\frac{H^*}{a_2}=1+\frac{\lambda kz}{a_2}+\phi\sin\,2\pi(z-ct),\ E_1=-\frac{\sigma a_2^3}{\lambda^3\,\mu\, c}, E_2=-\frac{m\, a_2^3\, c}{\lambda^3\,\mu},$$

$$E_3=-\frac{a_2^3\, c}{\lambda^2\,\mu}, \kappa=\frac{a_2\,\eta_d}{k_1},\quad Br=\frac{\eta_d\, c^2}{{a_2}^2\, T_0^*}. \tag{2.9}$$

Where δ is the wavenumber, ϕ is the amplitude ratio, Br is the Brinkman number is respectively. With the aid of Eq. (2.9) and the constraints of a $\delta \ll 1$ and (R e=0), Eqs. (2.3)-(2.8) have the following form.

$$\frac{1}{r}\frac{\partial(r\, u)}{\partial r}+\frac{\partial w}{\partial z}=0, \tag{2.10}$$

$$\frac{\partial p}{\partial r}=0, \tag{2.11}$$

$$\frac{\partial p}{\partial z}=\frac{1}{r}\frac{\partial(r\tau_{rz})}{\partial r}, \tag{2.12}$$

$$\left[\frac{1}{r}\frac{\partial\theta}{\partial r}+\frac{\partial^2\theta}{\partial r^2}\right]=-B_r\tau_{rz}\left(\frac{\partial w}{\partial r}\right), \tag{2.13}$$

$$\frac{\partial w}{\partial r} = 0 \; at \; r = 0, \;\; w = -1 + \beta \frac{\partial w}{\partial r} \;\; at \; r = h, \tag{2.14}$$

$$\frac{\partial \theta}{\partial r} + \kappa\theta = 0 \; at \; r = h, \; \frac{\partial \theta}{\partial r} = 0 \;\; at \; r = 0. \tag{2.15}$$

The basic non-dimensional equation for a Jeffrey fluid is stated by (Hanumesh Vaidya (2017))

$$\tau_{rz} = \frac{1}{1+\lambda_1}\frac{\partial w}{\partial r}. \tag{2.16}$$

The governing mathematical expression of a flexible wall can be attributed as (Kumar et al (2013), Srinivas et al (2010)

$$L(H^*) = p^* - p_0. \tag{2.17}$$

The operator L describes the flow of the stretched membrane, such that

$$L = -\sigma\frac{\partial^2}{\partial z^{*2}} + m\frac{\partial^2}{\partial t^{*2}} + C\frac{\partial}{\partial t^*}, \tag{2.18}$$

Furthermore, we may infer that $p_0 = 0$ since p_0 depicts the pressure applied on the wall surface outside due to muscle strain. It becomes dimensionless afterward.

$$\frac{\partial p}{\partial z} = \frac{\partial L(h)}{\partial z} = E_1\frac{\partial^3 h}{\partial z^{*3}} + E_2\frac{\partial^3 h}{\partial z \partial t^{*2}} + E_3\frac{\partial^2 h}{\partial z^* \partial t^*} = A(z,t). \tag{2.19}$$

II. Analytical Solutions

The exact solution of Eqs. (2.12) and (2.13) by imposing the boundary conditions Eq. (2.14) and Eq. (2.15) is obtained as

$$w = \frac{(1+\lambda_1)\,A}{4}[(r^2 - h^2) + 2\,h\,\beta] - 1. \tag{3.1}$$

$$\theta = \frac{BrA^2(1+\lambda_1)}{64}\left[(h^4 - r^4) + \frac{4\,h^3}{\kappa}\right]. \tag{3.2}$$

The corresponding stream function can be obtained by using the formula

$$u = -\frac{1}{r}\frac{\partial \psi}{\partial z}, \;\; w = \frac{1}{r}\frac{\partial \psi}{\partial r}. \tag{3.3}$$

Plugging Eq. (22) into Eq. (20) and integrating, we get:

$$\psi = \frac{r^2}{16}\left(-8 + A(-2h^2 + r^2 + 4h\beta)(1+\lambda_1)\right). \tag{3.4}$$

Whereas

$$A(z,t) = \phi(-(2\pi)^3\mathrm{Cos}[2\pi(z-t)](E_1 + E_2) + E_3(2\pi)^2\mathrm{Sin}[2\pi(z-t)]). \tag{3.5}$$

III. Interpretation of Results

This section gives numerical simulations with the aid of graphs. We utilized the **Mathematica package** to see the numerical implications of the developing guideline in the current exploration outcomes**.**

1.1. Velocity Distribution

Figures 2(a)-2(e) are used to scrutinize the salient features of velocity, temperature distribution, and trapping phenomenon. The velocity distribution behavior for various values λ_1, E_1, E_2 is shown in the Figures. 2(a)-2(e). The amplitude of velocity components rises when the material parameter λ_1 is raised in Figure 2 (a)**,** whereas the behavior near the wall is the contrary. Figure 2(b) illustrates that as the slip parameter β is enhanced, velocity drops. Figures 2(c) and 2(d) indicated that increasing the value of E_1 and E_2 causes the fluid velocity to rise immediately. Figure 2(e) depicts the velocity curve for the damping nature of the wall E_3. With larger E_3 values, the velocity profile shows minor variability.

1.2. Temperature Distribution

Figures 3(a)-3(c) are graphed to observe the Impacts of different variables on the temperature. Figure 3(a) depicts the Impact of Br. Clearly with larger Brinkman number causes an increase in temperature. Brinkman number persuades the viscous dissipation effects influenced by the creation of energy and hence improves the temperature. The impact κ on temperature is depicted in Figure 3(b). It is noticed that the rising value κ leads to decay in temperature. The reason for this is that when the Biot number rises, the thermal conductivity declines, contributing to a lower temperature profile. Figure 3(c) displays the λ_1 effect on θ. In this case for a larger value of λ_1 the temperature rises. Figures 3(d) to 3(f) demonstrates the impact of the elasticity parameters, E_1, E_2, and E_3 on temperature distribution. It has been revealed that raising the values of the elasticity factors optimizes the temperature profile.

1.3. Trapping Phenomenon

Another intriguing aspect of peristaltic action is trapping. Under some situations, streamlines in the wave frame divide, trapping a bolus of fluid propelled forward at the wave speed by the peristaltic wave. For this reason, Figures 4(a)-4(e) have been plotted. Figure 4(a) shows that the extent and magnitude of stream bolus at the top and lower walls increases as the Jeffrey fluid parameter raises. Figure 4(b) exhibits the influence of β on non-uniform tube entrapment. As is raised, the number of trapping bolus is reduced.

Figure 4(c) depicts a stream plot with increasing stiffness parameter values. The number of streamlines and bolus increases as the stiffness parameter increases, showing that the fluid is being circulated. Figure 4 (d) depicts consistent findings when the stiffness parameter E_2 is swapped byE_1. For improving levels, the number of trapped boluses rises. Figure 4(e) exhibits that the size of the bolus significantly increases as the value of E_3 rises, however, the number of confined boluses stays unchanged.

When the viscous damping force parameter is raised, the contour plots for viscous fluid are shown in Figure 4(e). Although the number of confined boluses remains constant, the size of each trapped bolus increases significantly.

IV. Conclusion

The current research focuses on the peristaltic transport of Jeffrey liquid via a non-uniform tube under the influence of slip and heat. For velocity, temperature distribution, and streaming function, an exact solution is calculated. The flow characteristics and trapping phenomena are explored in this research for various relevant aspects of the problem. The following are the significant findings:

- For the slip and Jeffrey fluid parameters, the fluid velocity exhibits the opposite behaviour.
- velocity distribution is an increasing function of $E_1, E_2,$ *and* E_3.
- The Brinkman value causes a temperature profile to widen. More viscous dissipation effects are associated
- With higher Br values, which indicate that fluid temperature rises as a result of increased heat production induced by shear in the fluid.
- As κ grows, thermal conductivity declines, resulting in a decline in the temperature profile.

References

[1] Latham, T. W 1966 Fluid Motion in a Peristaltic Pump, M.Sc. Thesis. MIT Cambridge. M. A

[2] Shapiro, A. H., and Jaffrin, M. Y 1969 Peristaltic pumping with long wavelengths at low Reynolds number. Journal of Fluid Mechanics, 4: 799-825.

[3] Brasseur, J.G. and Corrsin, S.Lu N.Q 1987 The influence of a peripheral layer of different viscosity on peristaltic pumping with Newtonian fluids. Journal of Fluid Mechanics, 495–519.

[4] Vasudev, C 2011 Effect of Heat transfer on the peristaltic flow of a Jeffrey Fluid through a porous medium in a vertical channel. Journal of Basic Applied. Science Research, 751-758.

[5] Asha, S. K, and Sunitha, G 2019 Influence of thermal radiation on peristaltic blood flow of a Jeffrey fluid with double diffusion in the presence of gold nanoparticles. Information in Medicine Unlocked, 17: 100272.

[6] Asha ,S.K and Sunitha, G 2020 "Double diffusion on peristaltic flow of nanofluid under the influences of a magnetic field, porous medium, and thermal radiation". Engineering Reports, 1-19.

[7] Mansutti ,D. G. Pontrelli, K.and Rajagopal R, 1993 Steady flows of non-Newtonian fluids past a porous plate with suction or injection. International Journal of Numerical Method, 927-941.

[8] Naveed Imran, Tassaddiq, A. Sohail, M. Nasser, A.A. Javed, M. Khan, I. 2020 Influence of chemical reaction and mechanism of peristasis for the thermal distribution obeying slip constraints: Application to conductive transportation. Journal of Material Research and Technology, 9: 6533-6543.

[9] Gijabhare, B.P. Krishnaprasad, J. Mishra, S 2019 The peristaltic flow of Buongiorno model nanofluids within a sinusoidal wall surface used in drug delivery. Heat Transfer-Asian Research, 1-19.

[10] Narula, V.K. Tripathi, D 2020 Entropy and exergy analysis on parasitic pumping in a curved narrow Channel. Heat Transfer Asian Research**,** 1-17.

[11] Rathod, V.P. Mahadev, M 2011 Effect of thickness of the porous material on the peristaltic pumping of a Jeffrey fluid with non-erodible porous lining wall, International. Journal of Mathematical Archive, 1-10.

[12] Maqbool, K. Shaheen, S. Mann, A. B 2016 Exact solution of cilia induced flow of a Jeffrey fluid in an inclined tube, Springer plus, 1379.

[13] Kavitha, A. Hemadri Reddy, R. Srinivas, A.N.S. Sreenadh, S. Saravana, R 2012 Peristaltic transport of a Jeffrey fluid between porous walls with suction and injection. International Journal of Mechanical and Material Engineering,152–157.

[14] Hanumesh Vaidya 2017 Influence of velocity slip and heat transfer on peristaltic transport of Jeffery fluid in an inclined elastic tube. "International Journal of creative research thoughts, 288-302

[15] Nadeem,S. Arshad Riaz, Ellahi, R 2013 Peristaltic flow of a Jeffrey fluid in a rectangular duct having compliant walls. Chemical Industrial Chemical Engineering Quarterly, 399–409.

[16] Akram,S. Zafar, S. Nadeem 2 018 Peristaltic transport of a Jeffrey fluid with double-diffusive convection in Nanofluids in the presence of an inclined magnetic field. International Journal of Geometric Method in Modern Physics, 1850-181

[17] Singh, U. P. Amit Medhavi, Gupta, R. S. Siddarth Shanker Bhatt 2018 Theoretical study on heat transfer on peristaltic transport of Non-Newtonian Fluid flowing in a channel: Rabinowistch fluid model. International Journal of Mathematical, Engineering and Management Sciences, 3: 2018.

[18] Hayat, T. Hina, T 2011 Effects of heat and mass transfer on peristaltic flow of Williamson fluid in a non-uniform channel with slip conditions. International Journal of Numerical Methods in Fluids, 1590-1604

[19] Rathod, V.P. Mahadev, and M 2012 The peristaltic flow of Jeffrey fluid with slip effects in an inclined channel. Journal of Chemical, Biological, Physical Sciences, 1987- 1997.

[20] Hayat, T. Qureshi, M. Ali, N 2007 The influence of slip on the peristaltic motion of a third-order fluid in an asymmetric channel. Physics Letter. A, 2653-2664.

[21] Ali, N. Wang,Y. Hayat,T. Oberlack.M 2009 Slip Effects on the peristaltic flow of a third-grade fluid in a circular cylindrical tube. Journal of Applied Mechanics, 1-10.

[22] Srinivas, S. Gayathri, R. Kothandapani, M 2009 The influence of slip conditions, wall properties and heat transfer on MHD peristaltic transport. Computer Physics Communication, 2115–2122

[23] Srinivas, S. Muthuraj, R 2010 Peristaltic transport of a Jeffrey fluid under the effect of slip in an inclined asymmetric channel. International Journal of Applied Mechanics, 437- 455.

[24] Rathod, V.P. Mahadev, M 2014 Effect of heat transfer on the peristaltic MHD flow of a Jeffrey fluid in an inclined channel. International Journal of Innovative Technology and Creative Engineering, 180-190.

[25] Rathod, V.P. Mahadev, M 2014 Interaction of heat transfer and peristaltic pumping of frictional second-grade fluid through a vertical cylindrical tube. Thermal Science, 18: 1109-1118.

[26] Rathod, V.P. Channakote, M.M 2011 A study of ureteral peristalsis in the cylindrical tube through a porous medium. Advance Applied Science Research, 134-140.

[27] Wahed, M. Hasona, Abdelhafeez, El-Shekhipy, M.G "Ibrahim, 2019 Semi-analytical solution to MHD The peristaltic flow of a Jeffrey fluid in presence of Joule heat effect by using the multi-step differential transform method. New Trends in Mathematical Science, 123-127.

[28] Asha, S. K. Deepa, C. K 2014 Impacts of the hall and heat transfer on peristaltic blood flow of an MHD Jeffrey fluid in a vertical asymmetric porous channel. International Journal of Advances in Applied Mathematics and Mechanics, 55-63.

[29] Channakote, M.M. Kalse, V.D 2021 Heat transfer in peristaltic motion of Rabinowistch fluid in a channel with a permeable wall. Applications Applied Mathematics, 16: 1057-1076.

[30] Thanesh Kumar, K. Kavitha, 2017 The influence of slip effect on peristaltic transport of a Rabinowitsch fluid model in a non-uniform tube. Material science Engineering, 263: 062004.

[31] Hina, S. Nadeem, S. 2017 Analysis of combined convective and viscous dissipation effects for Peristaltic flow of Rabinowitsch fluid Model. Journal of Bionic Engineering, 14: 182-190.

[32] Kumar, K.A, Sreenadh, S. Srinivas, A.N.S 2013 Effects of wall properties and heat transfer on the peristaltic transport of a Jeffrey fluid in a channel. Advances in Applied Science Research, 159-172.

Appendix

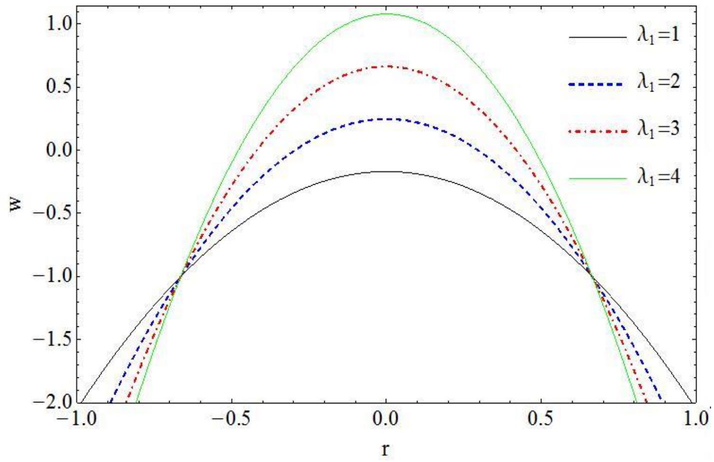

(a)

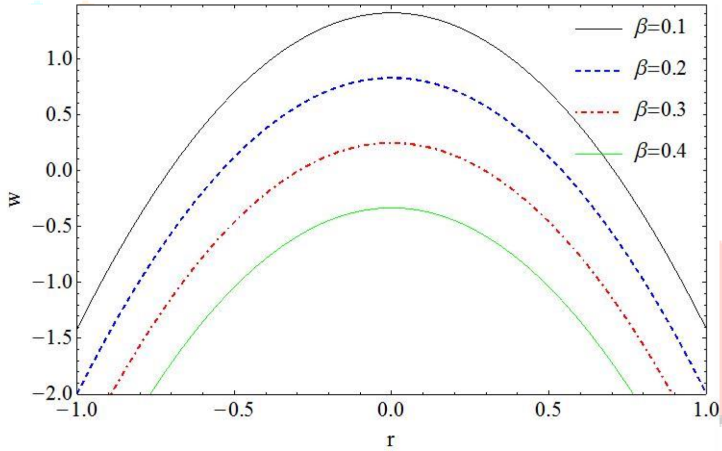

(b)

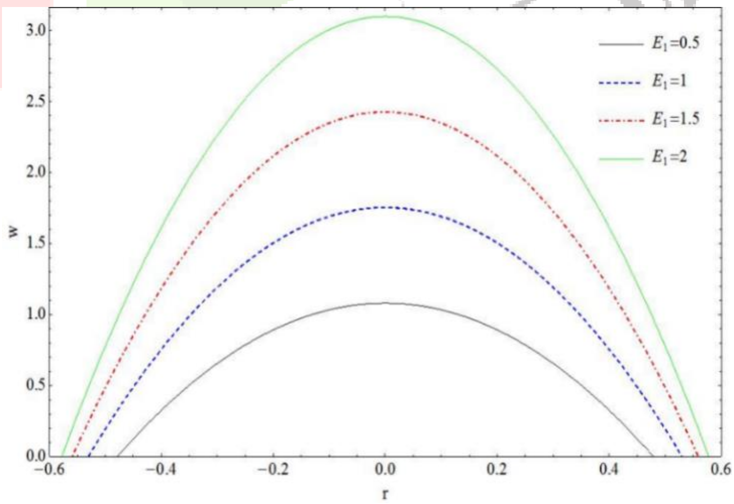

(c)

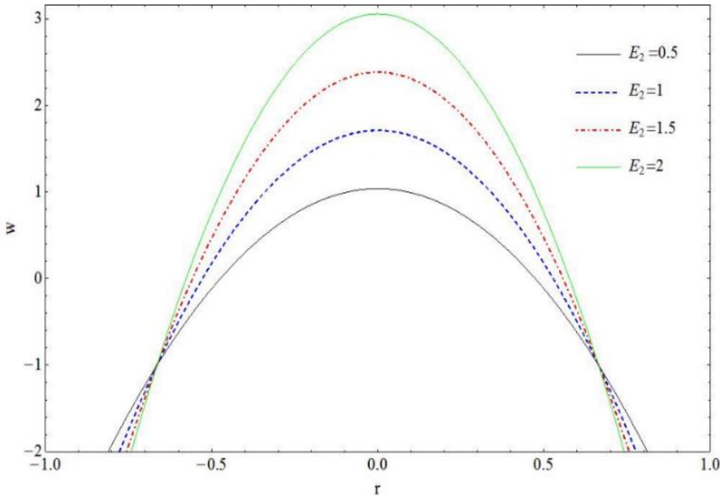

(d)

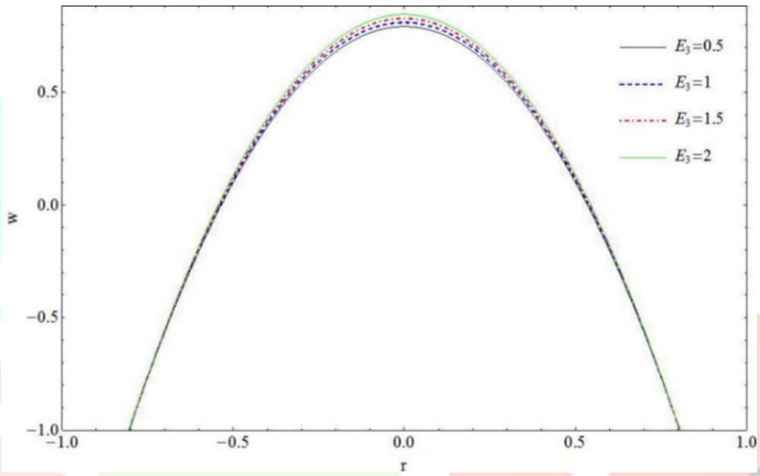

(e)

Figure 2. Impact of w on r for distinct (a) Jeffrey fluid parameter (λ_1), (b) Slip parameter β, (c) Rigidity parameter (E_1) (d) Stiffness parameter (E_2), (e) viscous damping force parameter(E_3).

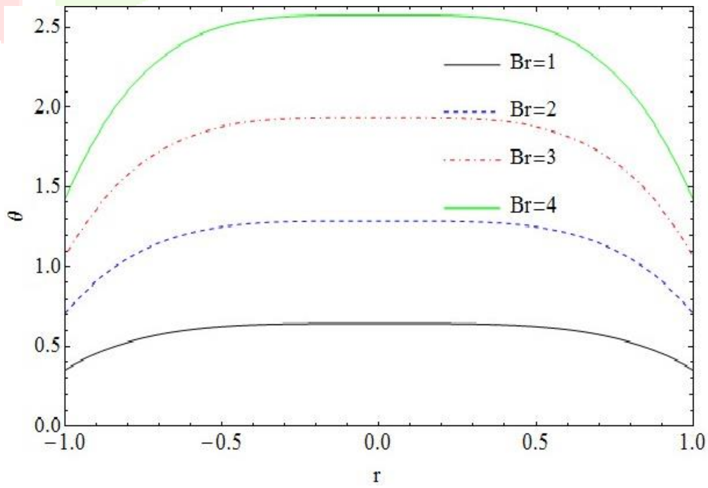

(a)

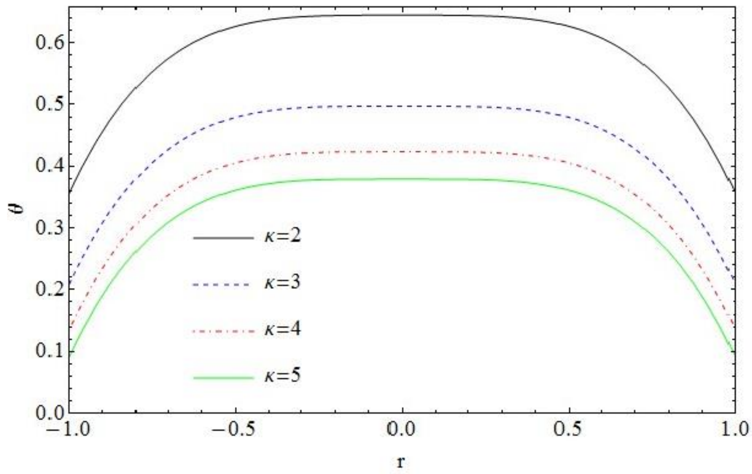
θ
0.6
0.5
0.4
0.3
0.2
0.1
0.0
κ=2
κ=3
κ=4
κ=5
−1.0
−0.5
0.0
0.5
1.0
r

(b)

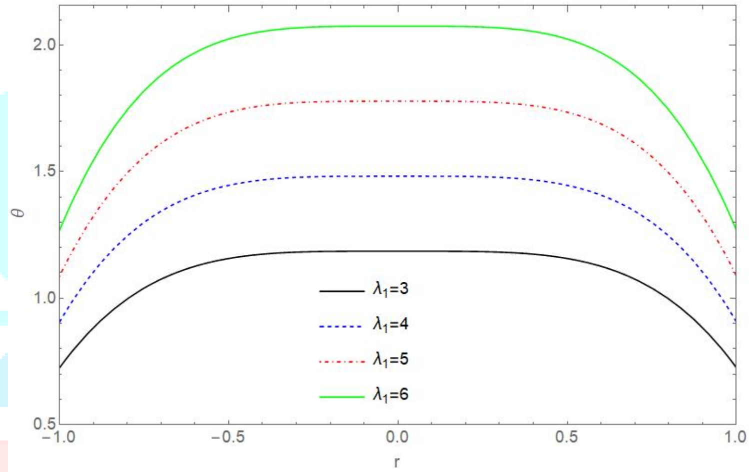
θ
2.0
1.5
1.0
0.5
λ1=3
λ1=4
λ1=5
λ1=6
−1.0
−0.5
0.0
0.5
1.0
r

(c)

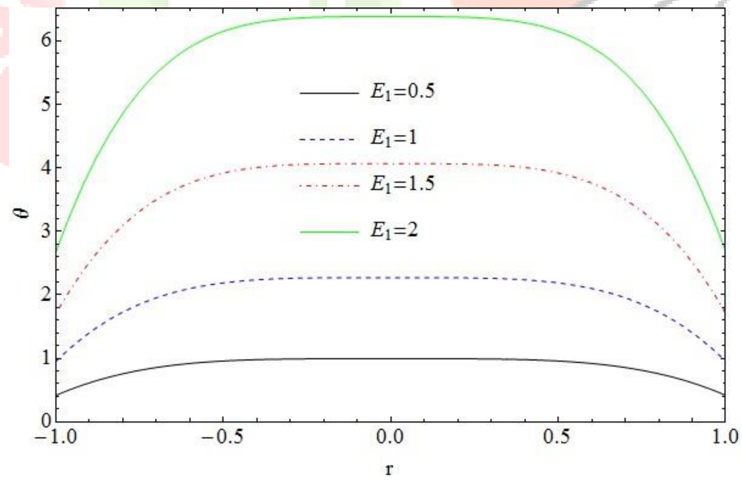
θ
6
5
4
3
2
1
0
E1=0.5
E1=1
E1=1.5
E1=2
−1.0
−0.5
0.0
0.5
1.0
r

(d)

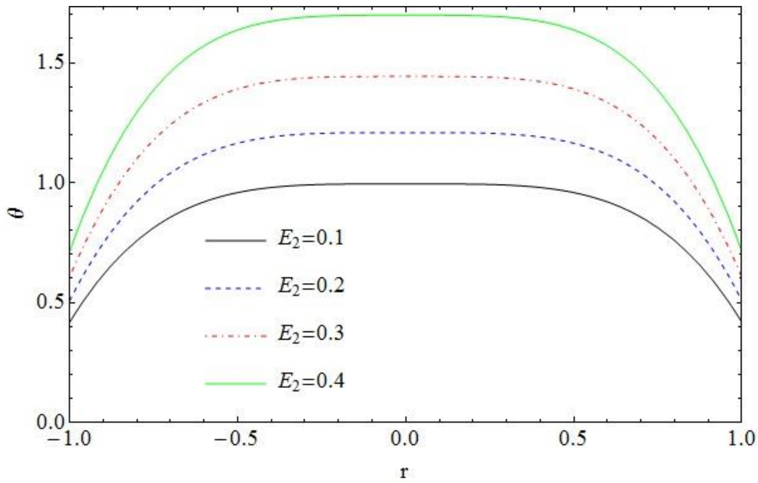

(e)

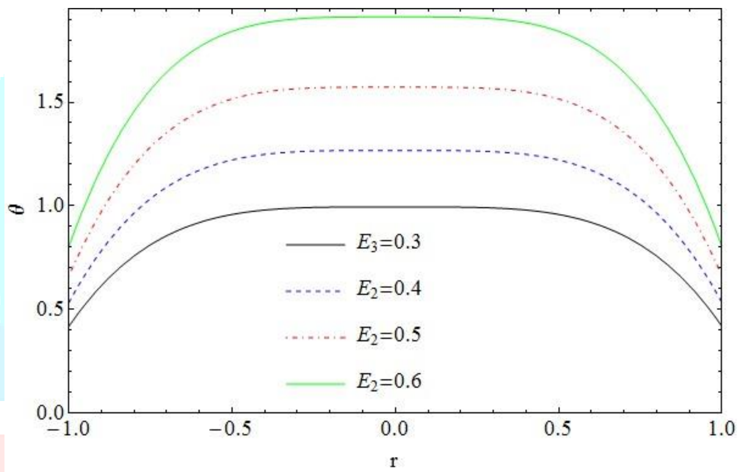

(f)

Figure 3. Impact of θ on r for distinct (a) Brinkman number Br, (b) Biot number κ, (c) Jeffrey fluid parameter (λ_1) , (d) Rigidity parameter E_1 (e) Stiffness parameter E_2, (f) viscous damping force parameter (E_3)

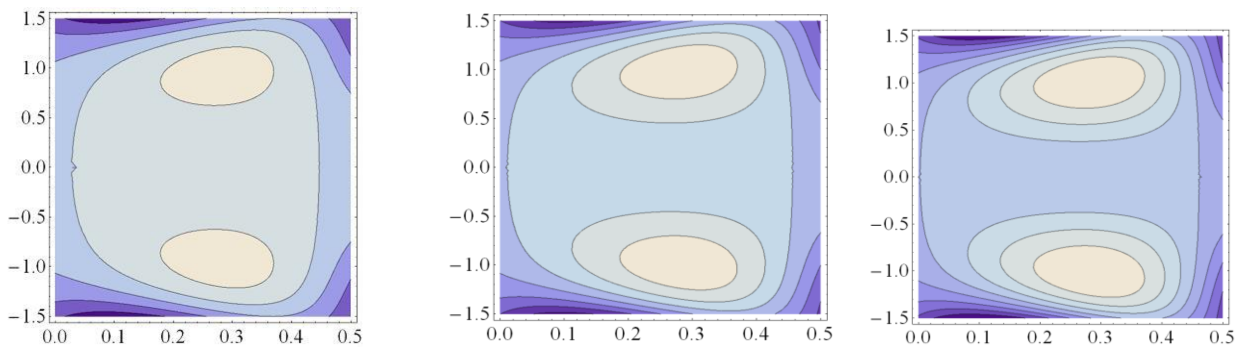

I. $\lambda_1 = 1$ II. $\lambda_1 = 2$ III. $\lambda_1 = 3$

Figure 4(a). Streamlines for different values of Jeffrey parameter (λ_1)

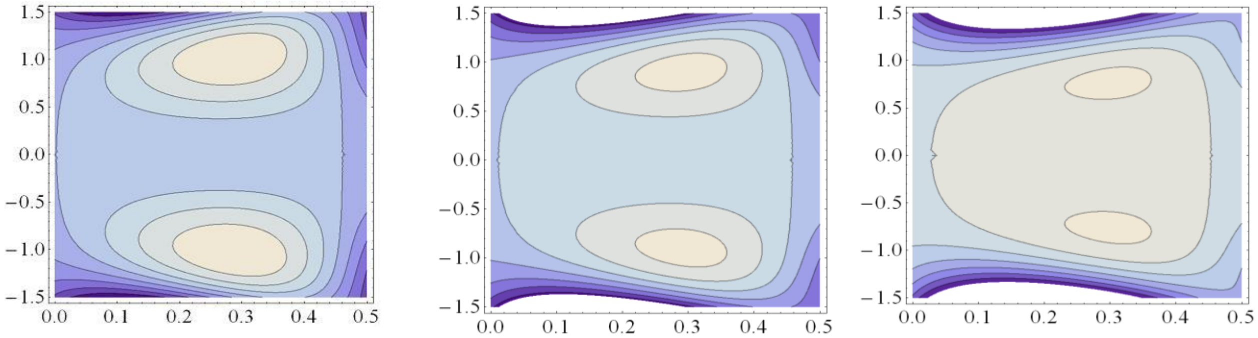

I. $\beta = 0.1$ II. $\beta = 0.2$ III. $\beta = 0.3$

Figure 4(b). Streamlines for different values of Slip parameter (β)

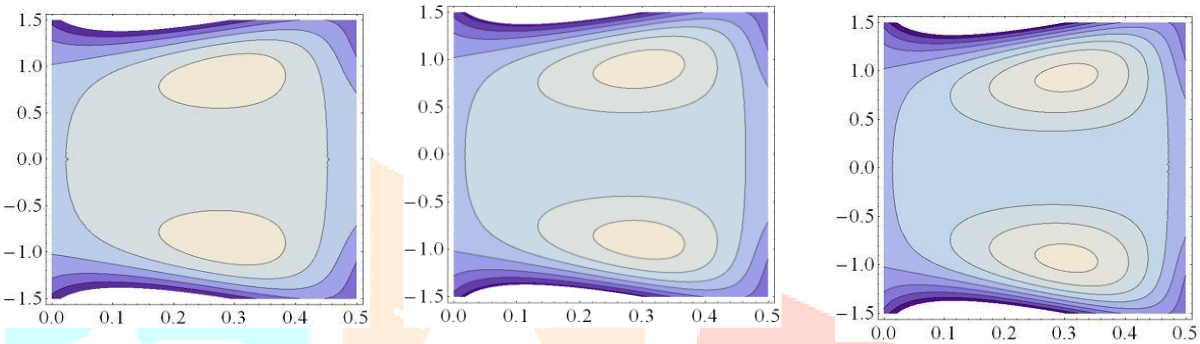

I. $E_1 = 0.4$ II. $E_1 = 1.1$ III $E_1 = 1.6$

Figure 4(c). Streamlines for different values of Rigidity parameter (E_1)

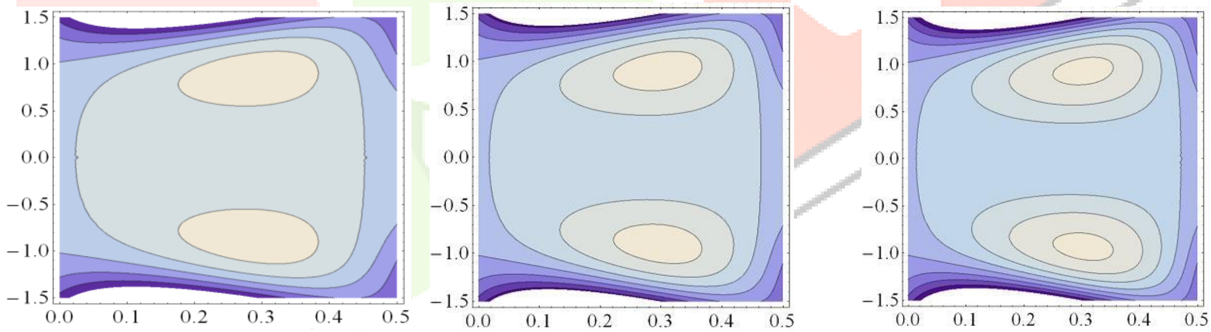

I. $E_2 = 0.4$ II. $E_2 = 1.1$ III. $E_2 = 1.6$

Figure 4(d). Streamlines for different values of Stiffness parameter (E_2).

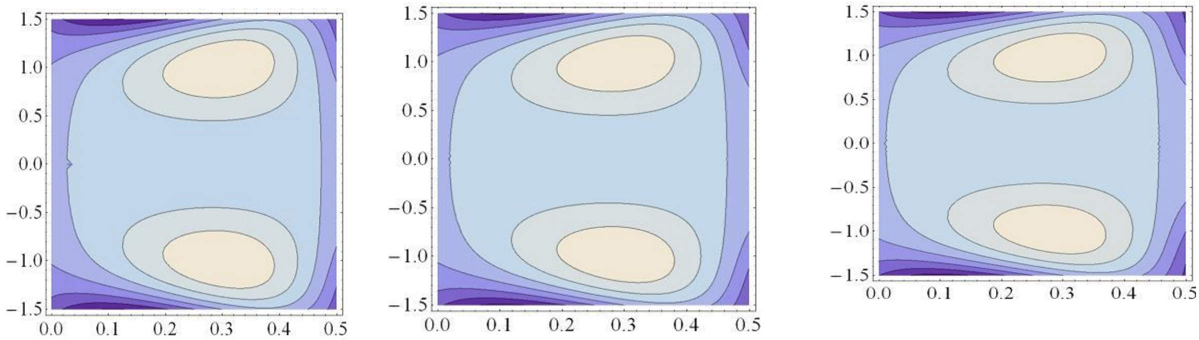

I. $E_3 = 0.4$ II. $E_3 = 1.1$ III. $E_3 = 1.6$

Figure 4(e). Streamlines for different values of Viscous damping parameter (E_3).